International Journal of Computational and Experimental Science and ENgineering (IJCESEN)

Vol. 11-No.4 (2025) pp. 9169-9180
http://www.ijcesen.com

ISSN: 2149-9144

Research Article

Marine Bastadins as Potent ACAT1 Inhibitors: Integrated Molecular Docking and ADMET Profiling for Anticancer Drug Discovery

Nabila Taib[1,2]*, Karim Ouadah[3,4], Khadidja Smail[5,6], Fatima Zohra Fadel[7,8], Noureddine Tchouar[9,10]

[1]Laboratory of Environmental Process Engineering (LIPE), Faculty of Chemistry, University of Science and Technology of Oran Mohamed Boudiaf, P.O. Box 1503, El Mnaouer, 31000 Oran, Algeria
[2]Department of Biotechnology, Faculty of Natural and Life Sciences, University of Science and Technology of Oran Mohamed Boudiaf, P.O. Box 1503, El Mnaouer, 31000 Oran, Algeria
*** Corresponding Author Email:** nabila.taib@univ-usto.dz- **ORCID:** 0009-0006-2667-7548

[3]Laboratory of Environmental Process Engineering (LIPE), Faculty of Chemistry, University of Science and Technology of Oran Mohamed Boudiaf, P.O. Box 1503, El Mnaouer, 31000 Oran, Algeria
[4]Department of Living and Environment, Faculty of Natural and Life Sciences, University of Science and Technology of Oran Mohamed Boudiaf, P.O. Box 1503, El Mnaouer, 31000 Oran, Algeria
Email: karim.ouadah@univ-usto.dz- **ORCID:** 0009-0002-2290-2809

[5]Laboratory of Environmental Process Engineering (LIPE), Faculty of Chemistry, University of Science and Technology of Oran Mohamed Boudiaf, P.O. Box 1503, El Mnaouer, 31000 Oran, Algeria
[6]Department of Biotechnology, Faculty of Natural and Life Sciences, University of Science and Technology of Oran Mohamed Boudiaf, P.O. Box 1503, El Mnaouer, 31000 Oran, Algeria
Email: khadidja.smail@univ-usto.dz- **ORCID:** 0009-0002-6308-4718

[7]Laboratory of Environmental Process Engineering (LIPE), Faculty of Chemistry, University of Science and Technology of Oran Mohamed Boudiaf, P.O. Box 1503, El Mnaouer, 31000 Oran, Algeria
[8]Department of Biotechnology, Faculty of Natural and Life Sciences, University of Science and Technology of Oran Mohamed Boudiaf, P.O. Box 1503, El Mnaouer, 31000 Oran, Algeria
Email: fatimazohra.fadel@univ-usto.dz- **ORCID:** 0009-0009-8288-7293

[9]Laboratory of Environmental Process Engineering (LIPE), Faculty of Chemistry, University of Science and Technology of Oran Mohamed Boudiaf, P.O. Box 1503, El Mnaouer, 31000 Oran, Algeria
[10]Department of Physical Chemistry, Faculty of Chemistry, University of Science and Technology of Oran Mohamed Boudiaf, P.O. Box 1503, El Mnaouer, 31000 Oran, Algeria
Email: noureddine.tchouar@univ-usto.dz- **ORCID**: 0009-0001-8389-0445

Article Info:

DOI: 10.22399/ijcesen.4378
Received : 15 March 2025
Revised : 10 October 2025
Accepted : 14 November 2025

Keywords

ACAT1;
Bastadins;
Cancer;
Molecular Docking;
ADMET

Abstract:

Acyl-CoA: cholesterol acyltransferase 1 (ACAT1) is a key enzyme in lipid homeostasis, catalyzing the esterification of cholesterol, a process closely associated with the metabolic reprogramming that supports tumor progression. In this study, twenty-two Bastadins, bromotyrosine-derived macrocyclic metabolites isolated from the marine sponge Ianthella basta, were evaluated as potential human ACAT1 inhibitors using molecular docking, ADME analysis, and toxicity predictions. These compounds were selected based on prior reports of their experimental ACAT1 inhibitory activity, underscoring their potential as lead scaffolds for enzyme modulation. Molecular docking was performed using PyRx (v0.8), and ADMET properties were evaluated with ADMETlab 3.0 and ProTox 3.0. Among the compounds, Bastadins 8, 10, 13, and 19 demonstrated the strongest affinities toward ACAT1 (-11.0 to -11.5 kcal/mol). Bastadin 13 exhibited the most stable complex formation (-11.5 kcal/mol), involving strong hydrogen bonds as well as π-π T-shaped and π-alkyl interactions with key residues, including His460 and Phe384. Similarly, Bastadin 19 displayed a high interaction energy (-11.4 kcal/mol), engaging in stable polar and hydrophobic contacts with residues such as His460, Trp420, Asn421, Phe254, and Tyr417. ADMET predictions indicated that both Bastadins 13 and 19 possess favorable pharmacokinetic properties,

including enhanced intestinal absorption, metabolic stability, and low predicted toxicity. Overall, these compounds emerge as the most promising ACAT1 inhibitors, combining strong binding, robust interactions with critical residues, and favorable ADMET characteristics, offering a rational framework for the development of novel anticancer agents, and providing a solid basis for further experimental validation and optimization in targeted cancer therapy.

1. Introduction

Cancer remains one of the leading causes of morbidity and mortality worldwide, characterized by uncontrolled cell proliferation, metabolic reprogramming, and resistance to apoptosis [1.2]. Among the multiple hallmarks of cancer, lipid metabolism reprogramming has attracted significant attention due to its essential role in sustaining tumor growth and survival [3.4]. Cholesterol, a key component of cellular membranes and signaling pathways, is often dysregulated in cancer cells, which exhibit increased uptake, synthesis, and storage of this lipid to support rapid proliferation [5].

A pivotal enzyme in cholesterol homeostasis is acyl-coenzyme A: cholesterol acyltransferase 1 (ACAT1), also known as sterol O-acyltransferase 1 (SOAT1), which catalyzes the esterification of free cholesterol into cholesteryl esters (CEs) stored in cytoplasmic lipid droplets [6,7]. Elevated ACAT1 activity has been associated with CE accumulation in various malignancies, including glioblastoma, prostate, breast, and pancreatic cancers [8,9]. This metabolic adaptation contributes to cancer cell survival, membrane remodeling, and chemoresistance by buffering the cytotoxic effects of excess free cholesterol, positioning ACAT1 as a promising metabolic target for anticancer therapy [10]. Recent studies have demonstrated that ACAT1 inhibition can suppress tumor cell proliferation, induce apoptosis, and sensitize cancer cells to chemotherapeutic agents [11]. Although several synthetic inhibitors have shown preclinical potential, their clinical translation remains limited due to pharmacokinetic and safety concerns [12]. Consequently, there is growing interest in identifying natural ACAT1 inhibitors with improved efficacy and biocompatibility [13].

Marine organisms, particularly sponges, are renowned for producing structurally diverse secondary metabolites with significant pharmacological potential [14,15]. Among these, Bastadins, bromotyrosine-derived macrocyclic compounds isolated from *Ianthella basta* [16], have received particular attention for their capacity to modulate lipid metabolism. The study by Eguchi et al. (2015) demonstrated, for the first time, that several Bastadins, including Bastadin 6, effectively suppress cholesteryl ester accumulation in macrophages, inhibit foam cell formation, and exhibit no toxicity at the tested concentrations [17]. Their work also identified a selective ACAT1 inhibitor among these compounds, establishing Bastadins as promising natural candidates for targeting lipid-associated disorders, including atherosclerosis and cancer [17,18]. In addition, Bastadins exhibit cytotoxic [19], anti-angiogenic [20], and antimigratory effects in cancer models [18], indicating a dual capacity to target both tumor growth and the lipid metabolic pathways that sustain it [21]. This multifaceted activity underscores their potential as candidates for anticancer therapies aimed at disrupting cholesterol esterification, a process increasingly recognized as essential for tumor proliferation, metastasis, and chemoresistance [10,22].

More recently, a computational screening and QSAR study conducted by Taib and Tchouar (2025) investigated the inhibitory activity of Bastadins against ACAT1, representing the first systematic theoretical analysis aimed at predicting their affinity and structural determinants [23]. Despite these advances, no computational study has yet elucidated the detailed molecular interaction mechanisms of Bastadins with ACAT1.

The primary aim of this study is to identify and characterize twenty-two Bastadins as potential ACAT1 inhibitors using molecular docking and ADMET simulations. Docking analyses are employed to elucidate the binding interactions with the ACAT1 active site, estimate binding affinities, and identify key residues involved in ligand recognition, providing insight into possible mechanisms of inhibition [24]. In parallel, ADMET evaluations assess pharmacokinetic and toxicity profiles to ensure that only candidates with favorable safety and efficacy characteristics are selected for further development [25]. By integrating these computational approaches, this work establishes a rational framework for the discovery of ACAT1 inhibitors and highlights their potential as targeted agents for disrupting cholesterol esterification in cancer, supporting the development of more effective and tailored anticancer therapies.

2. Materials and methods

2.1 Molecular Docking

A dataset consisting of twenty-two Bastadins was established, and their chemical structures were retrieved from the PubChem and ZINC databases [26,27]. The compounds were initially saved in SDF format to ensure compatibility with molecular docking software. Subsequently, ligand structures were energy-minimized and converted into PDBQT format using PyRx/OpenBabel for downstream docking analysis [28,29]. The three-dimensional crystal structure of human ACAT1 in complex with the inhibitor Nevanimibe (PDB ID: 6VUM) was obtained from the RCSB Protein Data Bank [30] for comparative docking studies. Protein preparation and optimization were performed in BIOVIA Discovery Studio (v24) [31], where water molecules, heteroatoms, and co-crystallized ligands were removed; polar hydrogens were added, nonpolar hydrogens merged, and charges assigned [28]. The receptor was then converted to PDBQT format using Auto Dock Vina tools [32].

Molecular docking was carried out with PyRx (v0.8), using the AutoDock Vina module [28], which included both re-docking of the co-crystallized ligand and docking of the twenty-two Bastadins. The docking grid was defined to cover the active site, with the macromolecule placed within a center-oriented grid box to allow flexible ligand binding. The grid box was centered at X = 155.163 Å, Y = 144.480 Å, Z = 148.644 Å, with dimensions of 26.063 × 15.756 × 23.174 Å along the X, Y, and Z axes.

To validate the docking protocol, the root-mean-square deviation (RMSD) between there-docked ligand and the co-crystallized ligand was calculated using PyMOL3.1, ensuring the reliability of the docking procedure [33,34]. Finally, protein-ligand interactions for all complexes were visualized using BIOVIA Discovery Studio Visualizer (v24) [35], and binding poses were assessed based on docking scores and RMSD values [36].

2.2 ADME Prediction

ADME (Absorption, Distribution, Metabolism, and Excretion) analysis was performed to assess the pharmacokinetic behavior of the selected Bastadins in relation to their molecular docking interactions with ACAT1. The predictions were generated using ADMETlab 3.0 [37], which provides an integrated evaluation of key pharmacokinetic parameters, including absorption efficiency, distribution potential, metabolic stability, and excretion characteristics. These computational assessments complemented the molecular docking outcomes by offering insights into the probability of each compound effectively reaching the target site, exhibiting optimal bioavailability, and maintaining favorable pharmacological properties [38].

2.3 Toxicity Analysis

Toxicological profiling of the selected Bastadins was performed using the ProTox 3.0 web server, which employs advanced machine learning algorithms to predict various toxicity endpoints, including acute oral toxicity (LD_{50}), toxicity class, and potential biological targets [39]. The molecular data of each compound were retrieved using their PubChem and Zinc identifiers, and subsequently processed through the ProTox 3.0 platform [40]. This predictive assessment, in conjunction with the molecular docking results, enabled the identification of Bastadins exhibiting strong binding affinity toward ACAT1 while maintaining a favorable and safe toxicity profile suitable for further pharmacological development.

3. Results and discussion

3.1 Molecular docking

Validation of the Molecular Docking Protocol

To verify the reliability of the docking protocol, a re-docking procedure was performed using the co-crystallized ligand from the PDB structure 6VUM. The ligand was reinserted into its native binding pocket to assess the ability of the docking algorithm to reproduce the experimentally observed binding conformation. This approach serves as a validation step, confirming the model's accuracy in predicting ligand-protein interactions.

The precision of the docking process was evaluated by calculating the root-mean-square deviation (RMSD) between the experimental and predicted poses. The obtained RMSD value of 1.80 Å demonstrates an excellent alignment, well below the commonly accepted 2 Å threshold, indicating a highly reliable docking performance.

As illustrated in Figure 1, the superposition of the docked (red) and co-crystallized (Green) ligands reveals an almost identical spatial orientation, further confirming the robustness and accuracy of the docking protocol.

3.2 Interactions of Bastadins with ACAT1

In the quest to identify novel inhibitors targeting 6VUM, it was crucial to elucidate the inhibition mechanism of the most promising compound emerging from the comprehensive screening process. A comparative assessment of the docking energies of all evaluated molecules revealed that several Bastadins exhibited more favorable binding affinities than the reference ligand, Nevanimibe, which registered a binding energy of -9.4 kcal/mol

(Table 1). These lower energies indicate that the Bastadins likely adopt more stable, energetically favorable poses within the enzyme's active site relative to the reference ligand.The molecular docking analysis provided detailed insights into the binding interactions of the reference ligand Nevanimibe and the selected compounds (Bastadin 8, 10, 13, and 19) within the active site of the ACAT1 enzyme. These four ligands were selected based on their high binding affinities, which ranged between (-11.0 and -11.5 kcal/mol), indicating stronger interactions with the target protein compared to other tested molecules.

The active site of ACAT1 is known to include eight key residues His460, Trp420, Asn421, Phe254, Phe258, Phe384, Tyr417 and Val424 [41], with His460 serving as the catalytic residue [41]. The analysis focused on identifying the nature and strength of ligand-residue interactions, their interatomic distances, and how these features correlate with the computed binding affinities. Overall, all tested Bastadin molecules displayed strong and specific interactions within the catalytic pocket of ACAT1, often surpassing the reference compound Nevanimibe in both interaction strength and predicted binding energy. To visualize the interactions of the reference ligand and the selected Bastadins within the 6VUM active site, BIOVIA Discovery Studio software was used. Figures 2 and 3 illustrate the binding interactions of the reference ligand and the top-scoring Bastadins within the ACAT1 active site.

For the reference ligand Nevanimibe, the binding affinity was recorded at -9.4 kcal/mol, and the docking pose revealed several stabilizing interactions with critical residues of ACAT1 (Table 2). Nevanimibe formed multiple conventional hydrogen bonds with His460 (2.55 Å), TRP420 (2.44 Å) and Asn421 (2.07 Å), as well as π-π stacking and π-alkyl interactions with Trp420, Phe258 and π-alkyl with His460, Phe384 and Val424. These short hydrogen-bond distances and aromatic contacts confirm that Nevanimibe occupies a highly favorable orientation within the active pocket, ensuring direct engagement with the catalytic residue His460. This interaction pattern is consistent with its known role as a potent ACAT1 inhibitor. The diversity and strength of these interactions validate the docking model and establish a reference framework for comparing the Bastadin compounds. Among the Bastadin molecules, Bastadin 8 exhibited a binding affinity of -11.1 kcal/mol, indicating stronger stabilization than Nevanimibe. This compound formed a carbon-hydrogen bond with His460 (2.97 Å), in addition to multiple π-alkyl interactions involving Phe254, Phe258, Phe384 and Tyr417. The combination of hydrophobic and aromatic interactions suggests that Bastadin 8 is deeply anchored in the enzyme's hydrophobic core. The presence of His460 among the interacting residues indicates that the ligand is correctly positioned within the catalytic pocket, making it a promising candidate for further inhibitory studies. Although its interaction profile is predominantly hydrophobic, the short H-bond distance with the catalytic histidine provides sufficient stability for effective inhibition. Bastadin 10 also demonstrated a strong binding affinity (-11.0 kcal/mol), stabilized by π-π and halogen interactions. It interacts with His460, Trp420, and Tyr417, forming π-alkyl and π-π T-shaped contacts in addition to a halogen bond at 3.00 Å. While the halogen bond contributes to specificity and electron-rich stabilization [42], the absence of strong hydrogen bonds may result in slightly reduced conformational stability compared to other derivatives [43]. Nevertheless, the halogen interaction is chemically meaningful, as bromine atoms often strengthen ligand-protein affinity through electrostatic complementarity [44]. Bastadin 10, therefore, exhibits a distinct binding mechanism driven mainly by hydrophobic and halogen contributions rather than hydrogen bonding. In contrast, Bastadin 13, which achieved the lowest binding energy (-11.5 kcal/mol), displayed the most favorable and biologically relevant interaction pattern. This compound formed two strong carbon-hydrogen bonds (1.97 Å and 2.45 Å) and a π-π T-shaped interaction (4.35 Å) with the catalytic residue His460, as well as additional stabilization with Phe384. The exceptionally short hydrogen-bond distances indicate a high degree of complementarity [45] between Bastadin 13 and the catalytic site, leading to a tight and energetically favorable complex. Its simultaneous engagement with His460 and an aromatic residue (Phe384) suggests a dual stabilization mechanism involving both hydrogen bonding and π–πT-shaped. This combination of interactions is typically associated with high-affinity binding and efficient inhibition, highlighting Bastadin 13 as the most promising derivative among all tested compounds. Similarly, Bastadin 19 showed a very strong binding affinity (-11.4 kcal/mol) and an extensive interaction network involving His460, Trp420, Asn421, Phe254, and Tyr417. The presence of both hydrogen bonds (3.01 Å) and π-π T-shaped interactions (4.78 Å) indicates a well-balanced interaction profile combining polar and hydrophobic contacts. The interaction with His460 again confirms correct positioning in the catalytic cavity, while the engagement with Trp420 and Asn421 mirrors the behavior of Nevanimibe.

The diversity of contacts suggests that Bastadin 19 benefits from multi-residue anchoring, enhancing overall complex stability even if the individual interactions are slightly weaker than those of Bastadin 13. Overall, the Bastadins tested here maintained direct contact with the catalytic residue His460, confirming that their binding modes overlap with the reference ligand Nevanimibe and thus likely share a similar inhibitory mechanism. The trend in binding affinities (Bastadin 13 > Bastadin 19 > Bastadin 8 > Bastadin 10 > Nevanimibe) correlates strongly with the density and strength of hydrogen bonding and aromatic stacking interactions. Bastadin 13 and Bastadin 19, in particular, stand out as the most promising inhibitors due to their high binding energies and well-oriented interactions with the catalytic site. These findings suggest that Bastadins could serve as potent and selective inhibitors of ACAT1, providing a structural basis for future optimization and experimental validation.

3.3 ADMET Prediction

In the process of drug development, numerous lead compounds are eliminated following docking studies, highlighting the importance of fulfilling ADMET (Absorption, Distribution, Metabolism, Excretion, and Toxicity) criteria for a compound to become a viable therapeutic agent [46]. These properties are crucial in assessing a molecule's potential for further development. The selected compounds were thoroughly evaluated for their ADMET characteristics, and the results are presented below.

The pharmacokinetic and toxicological parameters of Nevanimibe and the four selected Bastadin molecules (Bastadin 8, Bastadin 10, Bastadin 13 and Bastadin 19) were evaluated to assess their potential as safe and bioavailable ACAT1 inhibitors. Overall, the ADMET results reveal that all Bastadin compounds exhibit favorable pharmacokinetic characteristics and low toxicity, making them promising candidates for further development compared to the reference compound Nevanimibe.

3.4 ADME and Pharmacokinetic Analysis

In terms of absorption, Nevanimibe displayed a relatively low predicted human intestinal absorption (HIA) of 2.2%, whereas all Bastadin molecules demonstrated higher absorption values ranging between 2.8-14.7% (Table 3). Although these values remain modest, they suggest slightly improved permeability across intestinal barriers for the Bastadins, particularly Bastadin 19 (0.147%), which showed the highest predicted intestinal absorption. None of the Bastadin molecules were predicted to be P-glycoprotein (P-gp) inhibitors or substrates, indicating that they are unlikely to be affected by efflux transporters and may exhibit more consistent bioavailability compared to Nevanimibe, which is predicted to be a P-gp inhibitor. Additionally, none of the Bastadins were found to cross the blood-brain barrier (BBB), which is advantageous for ACAT1 inhibition since the target enzyme primarily acts in peripheral tissues such as the liver and macrophages. This reduced BBB permeability minimizes the risk of central nervous system side effects, including neurotoxicity.

Regarding metabolism, Nevanimibe was predicted to inhibit several cytochrome P450 (CYP) isoenzymes, including CYP1A2, CYP2D6, and CYP3A4, which may lead to potential drug-drug interactions and slower metabolism. In contrast, all Bastadin molecules were non-inhibitory toward the major CYP enzymes, implying they are less likely to interfere with hepatic metabolic pathways. This lack of CYP inhibition reflects a pharmacokinetically safer profile and suggests that Bastadins would not significantly alter the metabolism of co-administered drugs. Furthermore, their predicted total clearance (0.44-0.68 mL/min/kg) and half-life (1.85-2.44 h) values indicate a moderate elimination rate, consistent with compounds that remain bioactive for a reasonable duration without excessive accumulation in tissues.

3.5 Toxicological Assessments

The toxicity profile revealed notable differences between Nevanimibe and the Bastadin molecules. Nevanimibe was predicted to be neurotoxic, while all Bastadin compounds showed no hepatotoxicity, neurotoxicity, cardiotoxicity, carcinogenicity or cytotoxicity. This observation is significant, as neurotoxicity represents a major limitation for many lipophilic inhibitors that cross the BBB. The LD50 values further support the safety of the Bastadin molecules, ranging between 450-600 mg.kg-1, classified as Class 4, which indicates low acute toxicity. Although Nevanimibe exhibits a slightly higher LD_{50} (2100 mg.kg-1, class 5), its predicted neurotoxicity, P-gp inhibition and multiple CYP inhibitions suggest a less favorable safety profile. The absence of all major toxicological risks among the Bastadin derivatives strongly enhances their potential as safer ACAT1 inhibitors (Table 4).

Collectively, these results highlight that Bastadin 8, 10, 13 and 19 not only exhibit stronger binding

affinities for ACAT1 than the reference ligand but also possess cleaner pharmacokinetic and toxicity profiles. The lack of P-gp and CYP interactions implies that these compounds are less likely to cause drug-drug interactions or bioavailability issues. Among them, Bastadin 19 stands out due to its relatively higher intestinal absorption and low predicted toxicity, while Bastadin 13, the compound with the strongest binding affinity, also demonstrates acceptable pharmacokinetic behavior. Therefore, these Bastadin derivatives emerge as promising structural leads combining potent enzyme inhibition with favorable ADMET properties, warranting further in vitro and in vivo evaluation.

Figure 1. *Re-docking pose with the RMSD value of 1.80 Å (Green = Original, red = Docked).*

Table 1. *Docking energies of Bastadins studied as potential ACAT1 inhibitors*

ligands	ID	Affinity (kcal/mol)	ligands	ID	Affinity (kcal/mol)
Bastadin 1	ZINC ID : 150345721	-10.9	Bastadin 13	PubChem CID : 23426999	-11.5
Bastadin 2	PubChem CID : 53320792	-9.2	Bastadin 14	PubChem CID : 10260430	-9.8
Bastadin 3	ZINC ID : 150345724	-10.5	Bastadin 16	PubChem CID : 15965448	-10.8
Bastadin 4	PubChem CID : 10328662	-10.9	Bastadin 19	PubChem CID : 6413514	-11.4
Bastadin 5	PubChem CID : 6400637	-11.0	Bastadin 20	PubChem CID : 73210131	-10.3
Bastadin 6	PubChem CID : 9833337	-9.6	Bastadin 21	PubChem CID : 9579587	-10.9
Bastadin 7	PubChem CID : 10396070	-10.1	Bastadin 24	PubChem CID : 44448206	-9.2
Bastadin 8	PubChem CID : 6400643	-11.1	Bastadin 25	PubChem CID: 46848333	-8.7
Bastadin 10	PubChem CID : 11491539	-11.0	Bastadin 26	PubChem CID: 46848335	-9.6
Bastadin 11	ZINC ID : 169295671	-10	Hemibastadin 1	PubChem CID: 15338206	-9
Bastadin 12	PubChem CID : 44575628	-9.00	Hemibastadin 2	PubChem CID: 15338207	-9.3
Nevanimibe (reference ligand) : -9.4 (kcal/mol)					

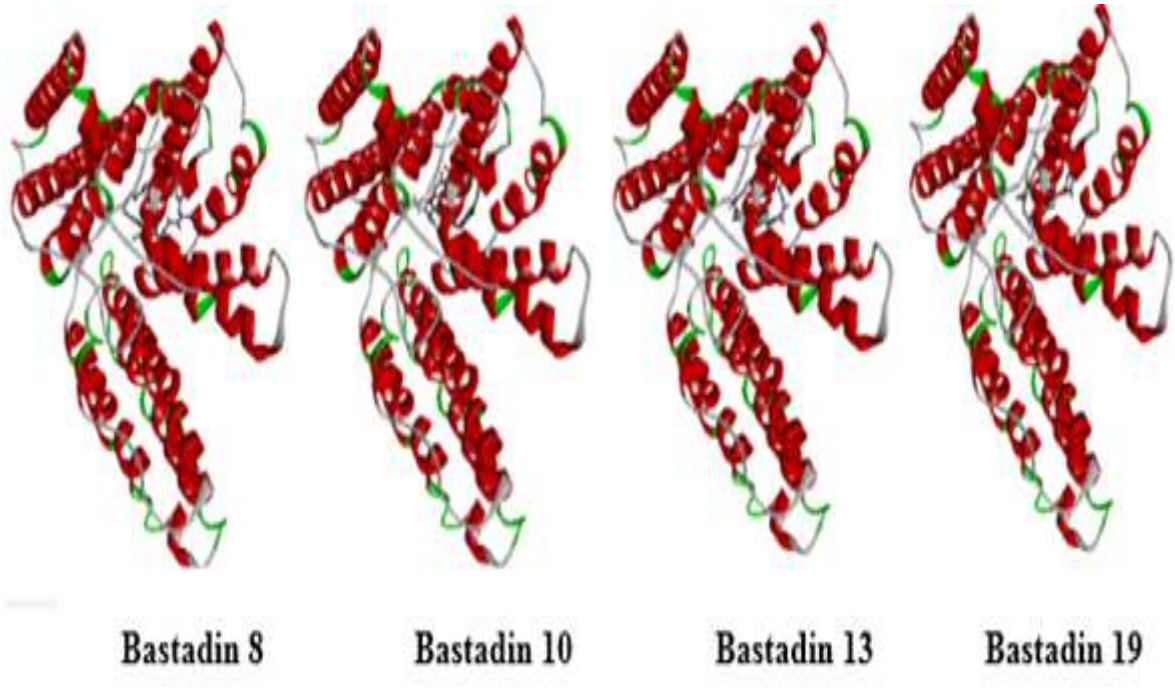

***Figure 2**. Binding interactions of Nevanimibe within the active site of ACAT1*

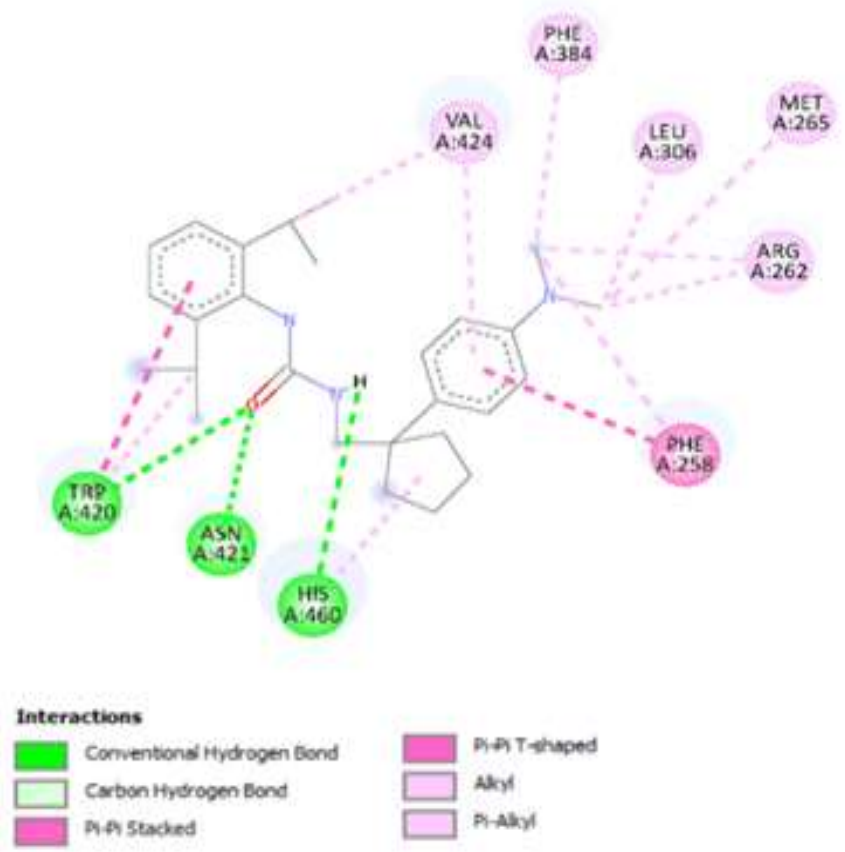

***Figure 3a.** Orientation of the Four Bastadins within the ACAT1 Active Site*

Ligands	Ligand-receptor interactions	Affinity (kcal/mol)
Bastadin 8	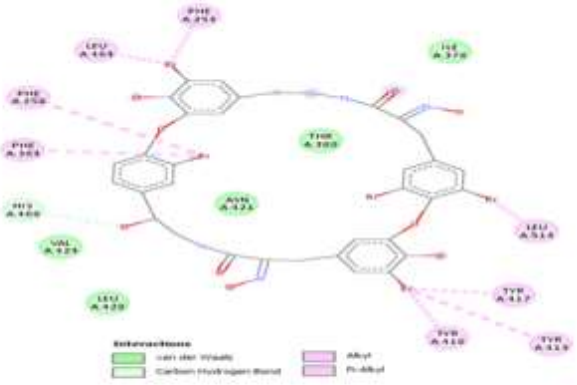	**-11.1**
Bastadin *10*	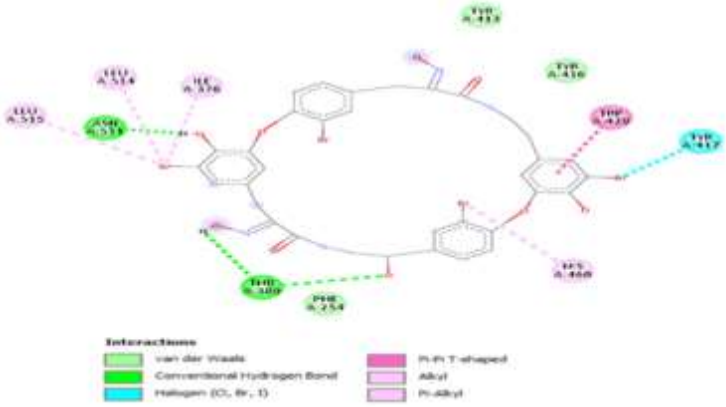	**-11.0**
Bastadin 13	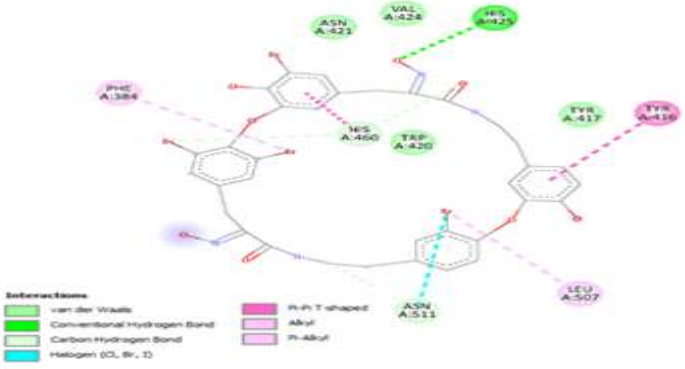	**-11.5**
Bastadin 19	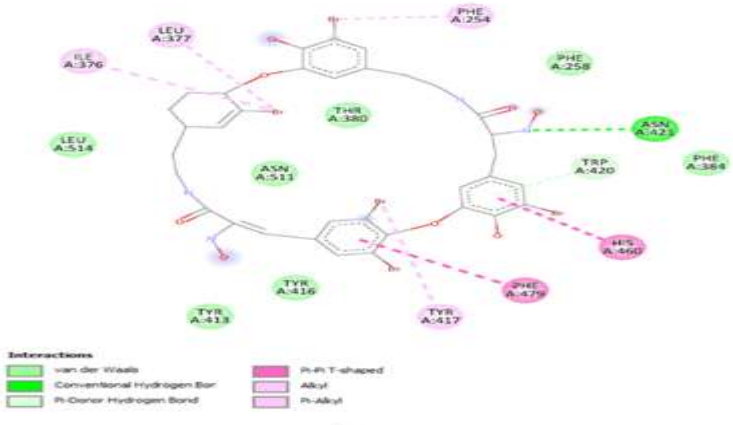	**-11.4**

Figure 3b. *2D Interaction Diagram of Bastadins with ACAT1*

Table 2. *Binding Interactions of Nevanimibe and Bastadins with ACAT1*

	Bond Type	Active Amino Acid	Bond Length (Å)
Nevanimibe	Conventional Hydrogen Bond	His460	2.55
	Pi-Alkyl		5.37
	Conventional Hydrogen Bond	Trp420	2.44
	Pi-Pi Stacked		4.39
	Pi-Alkyl		4.66
	Conventional Hydrogen Bond	Asn421	2.07
	Pi-Pi T-shaped	Phe258	4.69
	Pi-Alkyl		4.98
	Pi-Alkyl	Phe384	5.24
	Alkyl	Val424	4.33
	Pi-Alkyl		4.78
Bastadin 8	Carbon Hydrogen Bond	HIS460	2.97
	Pi-Alkyl	PHE254	5.48
	Pi-Alkyl	PHE258	4.81
	Pi-Alkyl	PHE384	4.14
	Pi-Alkyl	TYR417	4.28
Bastadin 10	Pi-Alkyl	HIS460	5.07
	Pi-Pi T-shaped	TRP420	5.13
	Halogen (Br)	TYR417	3.00
Bastadin 13	Pi-Pi T-shaped	HIS460	4.35
	Carbon Hydrogen Bond		1.97
	Carbon Hydrogen Bond		2.45
	Pi-Alkyl	PHE384	4.26
Bastadin 19	Pi-Pi T-shaped	HIS460	4.78
	Pi–Donor Hydrogen Bond	TRP420	3.15
	Conventional Hydrogen Bond	ASN421	3.01
	Pi-Alkyl	PHE254	4.42
	Pi-Alkyl	TYR417	5.16

Table 3. *Pharmacokinetics Parameters of Nevanimibe and Bastadins, Computed by ADMETlab*

Toxicity	Nevanimibe	Bastadin 8	Bastadin 10	Bastadin 13	Bastadin 19
Hepatotoxicity	Inactive	Inactive	Inactive	Inactive	Inactive
Neurotoxicity	Active	Inactive	Inactive	Inactive	Inactive
Cardiotoxicity	Inactive	Inactive	Inactive	Inactive	Inactive
Carcinogenicity	Inactive	Inactive	Inactive	Inactive	Inactive
Cytotoxicity	Inactive	Inactive	Inactive	Inactive	Inactive
LD50 (mg/kg)	2100	600	600	450	450
class	5	4	4	4	4

Table 4. *Toxicity prediction of Nevanimibe and molecules candidates*

Parameters	Nevanimibe	Bastadin 8	Bastadin 10	Bastadin 13	Bastadin 19
Human Intestinal Absorption (%)	2.2	5.2	2.8	13.5	14.7
P-gp Inhibitor	Yes	No	No	No	No
P-gp Substrate	No	No	No	No	No
Blood-Brain Barrier (BBB)	No	No	No	No	No
CYP1A2 Inhibitor	No	No	No	No	No
CYP2C19 Inhibitor	Yes	No	No	No	No

CYP2C9 Inhibitor	No	No	No	No	No
CYP2D6 Inhibitor	Yes	No	No	No	No
CYP3A4 Inhibitor	Yes	No	No	No	No
Total Clearance (CLtotal)	6.686	0.44	0.528	0.688	0.484
Half-life (T½)	0.469	2.439	2.284	1.855	2.244

4. Conclusions

This study provides an integrated evaluation of Bastadins as ACAT1 inhibitors, combining molecular docking, ADME profiling, and toxicity prediction to assess their pharmacological potential. Among the twenty-two derivatives analyzed, Bastadins 13 and 19 emerged as the most promising candidates, exhibiting the highest binding affinities (-11.5 and -11.4 kcal/mol, respectively). Docking analysis revealed that Bastadin 13 forms strong interactions with key catalytic residues, including His460 and Phe384, through hydrogen bonds, π-π T-shaped, and π-alkyl interactions, whereas Bastadin 19 forms a well-orchestrated network of hydrogen bonds and hydrophobic interactions, including π-π T-shaped contacts with His460, Trp420, Asn421, Phe254, and Tyr417, thereby promoting effective stabilization of the ligand within the enzyme's catalytic pocket. In silico ADME and toxicity predictions further supported their pharmacological suitability. Both compounds displayed superior intestinal permeability and did not interact with P-glycoprotein, minimizing the risk of efflux-mediated bioavailability reduction. They were also predicted to be unable to cross the blood-brain barrier, reducing potential central nervous system side effects. Neither inhibited key cytochrome P450 isoenzymes (CYP1A2, CYP2C19, CYP2C9, CYP2D6, CYP3A4), suggesting a low likelihood of metabolic interference or drug-drug interactions. Moderate clearance rates and prolonged half-lives indicate favorable systemic retention and metabolic stability, while toxicity predictions revealed no hepatotoxic, neurotoxic, cardiotoxic, or carcinogenic risks.

Collectively, these findings highlight Bastadins 13 and 19 as potent and safe ACAT1 inhibitors, supporting their further preclinical development. Their strong binding affinities, specific interactions with key catalytic residues, and favorable pharmacokinetic and safety profiles make them promising lead compounds. The integration of molecular docking, ADME profiling, and toxicity prediction provides a robust framework for rational optimization. Given ACAT1's role in lipid metabolism, these compounds hold potential for therapeutic applications in lipid-related disorders and cancer, warranting experimental validation and preclinical evaluation.

Author Statements:

- **Ethical approval:** The conducted research is not related to either human or animal use.
- **Conflict of interest:** The authors declare that they have no known competing financial interests or personal relationships that could have appeared to influence the work reported in this paper
- **Acknowledgement:** The authors declare that they have nobody or no-company to acknowledge.
- **Author contributions:** The authors declare that they have equal right on this paper.
- **Funding information:** The authors declare that there is no funding to be acknowledged.
- **Data availability statement:** The data that support the findings of this study are available on request from the corresponding author. The data are not publicly available due to privacy or ethical restrictions.

References

[1] Tufail, M., Wang, H., Wang, Y. (2024). Hallmarks of cancer resistance. Cell Death & Disease, 15, 266. https://pmc.ncbi.nlm.nih.gov/articles/PMC11145355/

[2] Schiliro, C., Firestein, B. L. (2021). Mechanisms of metabolic reprogramming in cancer cells supporting enhanced growth and proliferation. Cells, 10(5), 1056. https://doi.org/10.3390/cells10051056

[3] Cheng, C., Geng, F., Cheng, X., Guo, D. (2018). Lipid metabolism reprogramming and its potential targets in cancer. Cancer Communications, 38(1), 27. https://doi.org/10.1186/s40880-018-0301-4

[4] Terry, A. R., Hay, N. (2024). Emerging targets in lipid metabolism for cancer therapy. Trends in Pharmacological Sciences, 45(6), 537-551. https://doi.org/10.1016/j.tips.2024.04.007

[5] Mordzińska-Rak, A., Verdeil, G., Hamon, Y., Błaszczak, E., Tromb, T. (2025). Dysregulation of cholesterol homeostasis in cancer pathogenesis. Cellular and Molecular Life Sciences, 82(1), 168. https://doi.org/10.1007/s00018-025-05617-9

[6] Tu, T., Zhang, H., Xu, H. (2023). Targeting sterol-O-acyltransferase 1 to disrupt cholesterol metabolism for cancer therapy. Frontiers in Oncology, 13, Article 1197502. https://doi.org/10.3389/fonc.2023.1197502

[7] Bairos, J. A., Chinedu, U. N., Zafar, M., Akl, M. G., Li, L., Parlakgul, G., Arruda, A. P., Widenmaier, S. B. (2024). Sterol O-acyltransferase (SOAT/ACAT) activity is required to form cholesterol crystals in hepatocyte lipid droplets. Biochimica et Biophysica Acta (BBA) - Molecular and Cell Biology of Lipids, 1869(4), 159512. https://doi.org/10.1016/j.bbalip.2024.159512

[8] Ayyagari, V. N., Bandyopadhyay, A., Harris, R. E. (2020). Assessment of acyl-CoA:cholesterol acyltransferase-1 (ACAT-1) mediated cholesterol ester accumulation in ovarian cancer progression. PLOS ONE, 15(8), e0228024. https://doi.org/10.1371/journal.pone.0228024

[9] Zixi, S., Liu, Y., Yang, Y. (2024). Targeting ACAT1 in cancer: From threat to treatment. Frontiers in Oncology, 14, 1395192. https://doi.org/10.3389/fonc.2024.1395192

[10] Li, J., Gu, D., Lee, S. Y., Wang, X., Yang, Y., Liu, Q. (2016). Abrogating cholesterol esterification suppresses growth and metastasis of pancreatic cancer. Oncogene, 35 (25), 3343-3353. https://doi.org/10.1038/onc.2016.168

[11] He, W., Li, Y., Liu, S.-B., Chang, Y., Han, S., Han, X., Ma, Z., Amin, H. M., Song, Y.-H., Zhou, J. (2024). From mitochondria to tumor suppression: ACAT1's crucial role in gastric cancer. Frontiers in Immunology, 15, Article 1449525. https://doi.org/10.3389/fimmu.2024.1449525

[12] Sun, T., Xiao, X. (2024). Targeting ACAT1 in cancer: From threat to treatment. Frontiers in Oncology, 14, 1395192. https://doi.org/10.3389/fonc.2024.1395192

[13] Zhang, J. (2024). Target fishing and mechanistic insights of the natural anticancer drug candidate chlorogenic acid. Acta Pharmaceutica Sinica B, 14(10), 4431-4442. https://doi.org/10.1016/j.apsb.2024.07.005

[14] Yang, Q.-B., Liang, L.-F. (2024). Spongia sponges: Unabated sources of novel secondary metabolites. Marine Drugs, 22(5), 213. https://doi.org/10.3390/md22050213

[15] Raymond, M. J. F., Rakotondraibe, H. L. (2025). Recent updates on terpenoids and other bioactive constituents of marine sponges. Molecules, 30(5), 1112. https://doi.org/10.3390/molecules30051112

[16] Kazlauskas, R., Lidgard, R. O., Murphy, P. T., Wells, R. J., Blount, J. F. (1981). Brominated tyrosine-derived metabolites from the sponge Ianthella basta. Australian Journal of Chemistry, 34(4), 765-786. https://doi.org/10.1071/CH9810765

[17] Eguchi, K., Kato, H., Fujiwara, Y., Losung, F., Mangindaan, R. E. P., de Voogd, N. J., Takeya, M., Tsukamoto, S. (2015). Bastadins, brominated-tyrosine derivatives, suppress accumulation of cholesterol ester in macrophages. Bioorganic & Medicinal Chemistry Letters, 25(22), 5389-5392. https://doi.org/10.1016/j.bmcl.2015.09.024

[18] Mathieu, V., Wauthoz, N., Lefranc, F., Niemann, H., Amighi, K., Kiss, R., Proksch, P. (2013). Cyclic versus hemi-bastadins: Pleiotropic anti-cancer effects from apoptosis to anti-angiogenic and anti-migratory effects. Molecules, 18(3), 3543-3561. https://doi.org/10.3390/molecules18033543

[19] Miao, S. C., Andersen, R. J., Allen, T. M. (1990). Cytotoxic metabolites from the sponge Ianthella basta collected in Papua New Guinea. Journal of Natural Products, 53(6), 1441-1446. https://doi.org/10.1021/np50072a007

[20] Aoki, S., Cho, S.-H., Ono, M., Kuwano, T., Nakao, S., Kuwano, M., Nakagawa, S., Gao, J.-Q., Mayumi, T., Shibuya, M., Kobayashi, M. (2006). Bastadin 6, a spongean brominated tyrosine derivative, inhibits tumor angiogenesis by inducing selective apoptosis to endothelial cells. Anti-Cancer Drugs, 17(3), 269-278. https://doi.org/10.1097/00001813-200603000-00005

[21] Greve, H., Kehraus, S., Krick, A., Kelter, G., Maier, A., Fiebig, H. H., Wright, A. D., König, G. M. (2008). Cytotoxic Bastadin 24 from the Australian Sponge Ianthella quadrangulata. Journal of Natural Products, 71(3), 309-312. https://doi.org/10.1021/np070373e

[22] Xiao, M., Xu, J., Wang, W., Zhang, B., Liu, J., Li, J., Xu, H., Zhao, Y., Yu, X., Shi, S. (2023). Functional significance of cholesterol metabolism in cancer: From threat to treatment. Experimental & Molecular Medicine, 55(9), 1982-1995. https://doi.org/10.1038/s12276-023-01079-w

[23] Taib, N., Tchouar, N. (2025). Computational screening and QSAR study of bastadins as ACAT1 inhibitors. International Journal of Computational and Experimental Science and Engineering, 11(4), 7270-7288. https://doi.org/10.22399/ijcesen.3994

[24] Wu, F., Zhou, Y., Li, L., Shen, X., Chen, G., Wang, X., Liang, X., Tan, M., Huang, Z. (2020). Computational approaches in preclinical studies on drug discovery and development. Frontiers in Chemistry, 8, 726. https://doi.org/10.3389/fchem.2020.00726

[25] Laeeq, S., Dubey, V. (2022). Computational prediction of ADMET properties of ACAT inhibitors for synthesis and pharmacological screening. International Journal of Health Sciences, 6 (S7), 2377-2388. https://doi.org/10.53730/ijhs.v6nS7.11866

[26] Kim, S., Chen, J., Cheng, T., Gindulyte, A., He, J., He, S., Li, Q., Shoemaker, B. A., Thiessen, P. A., Yu, B., Zaslavsky, L., Zhang, J., Bolton, E. E. (2021). PubChem in 2021: new data content and improved web interfaces. Nucleic Acids Research, 49(D1), D1388-D1395. https://doi.org/10.1093/nar/gkaa971

[27] Sterling, T., Irwin, J. J. (2015). ZINC 15 – ligand discovery for everyone. Journal of Chemical Information and Modeling, 55(11), 2324-2337. https://doi.org/10.1021/acs.jcim.5b00559

[28] Dallakyan, S., Olson, A. J. (2015). Small-Molecule Library Screening by Docking with PyRx. In J. E. Hempel (Ed.), Chemical Biology: Methods and Protocols (Methods in Molecular Biology, Vol.

1263, pp. 243-250). Springer. https://doi.org/10.1007/978-1-4939-2269-7_19

[29] O'Boyle, N. M., Banck, M., James, C. A., Morley, C., Vandermeersch, T., Hutchison, G. R. (2011). Open Babel: An open chemical toolbox. Journal of Cheminformatics, 3, 33. https://doi.org/10.1186/1758-2946-3-33

[30] Berman, H. M., Battistuz, T., Bhat, T. N., Bluhm, W. F., Bourne, P. E., Burkhardt, K., Zardecki, C. (2002). The Protein Data Bank. Acta Crystallographica Section D: Biological Crystallography, 58(6), 899-907. https://doi.org/10.1107/S0907444902003451

[31] BIOVIA. (2024). BIOVIA Discovery Studio (Version 2024). Dassault Systèmes. San Diego, CA, USA.

[32] Trott, O., Olson, A. J. (2010). AutoDock Vina: Improving the speed and accuracy of docking with a new scoring function, efficient optimization, and multithreading. Journal of Computational Chemistry, 31(2), 455-461. https://doi.org/10.1002/jcc.21334

[33] Yusuf, D., Davis, A. M., Kleywegt, G. J., Schmitt, S. (2008). An alternative method for the evaluation of docking performance: RSR vs RMSD. Journal of Chemical Information and Modeling, 48(7), 1411-1422. https://doi.org/10.1021/ci800084x

[34] Schrödinger, LLC. (2023). The PyMOL Molecular Graphics System, Version 3.1

[35] Dassault Systèmes BIOVIA. (2024). BIOVIA Discovery Studio Visualizer, Version 24

[36] Morris, G. M., Huey, R., Lindstrom, W., Sanner, M. F., Belew, R. K., Goodsell, D. S., Olson, A. J. (2009). AutoDock4 and AutoDockTools4: Automated docking with selective receptor flexibility. Journal of Computational Chemistry, 30(16), 2785-2791. https://doi.org/10.1002/jcc.21256

[37] Xiong, G., Wu, Z., Yi, J., Fu, L., Yang, Z., Hsieh, C., Yin, M., Zeng, X., Wu, C., Lu, A., Chen, X., Hou, T. (2024). ADMETlab 3.0: Integrating AI and PBPK models with extended usability and reliability for ADMET predictions. Nucleic Acids Research, 52(W1), W422-W431. https://doi.org/10.1093/nar/gkae236

[38] Yang, H., Lou, C., Sun, L., Li, J., Cai, Y., Wang, Z., Li, W., Liu, G., Tang, Y. (2019). admetSAR 2.0: web-service for prediction and optimization of chemical ADMET properties. Bioinformatics, 35(6), 1067-1069. https://doi.org/10.1093/bioinformatics/bty707

[39] Banerjee, P., Koutsoukas, A., Ecker, G. F. (2024). ProTox-3.0: A webserver for the prediction of toxicity of chemicals. Nucleic Acids Research, 52(W1), W513-W519. https://doi.org/10.1093/nar/gkae303

[40] Li, Q., Cheng, T., Wang, Y., Bryant, S. H. (2010). PubChem as a public resource for drug discovery. Drug Discovery Today, 15(23-24), 1052-1057. https://doi.org/10.1016/j.drudis.2010.10.003

[41] Long, T., Sun, Y., Hassan, A., Qi, X., Li, X. (2020). Structure of nevanimibe-bound tetrameric human ACAT1. Nature, 581(7808), 339-343. https://doi.org/10.1038/s41586-020-2295-8

[42] Lu, Y., Wang, Y., Zhu, W. (2010). Non-bonding interactions of organic halogens in biological systems: Implications for drug discovery and biomolecular design. Physical Chemistry Chemical Physics, 12(18), 4543-4551. https://doi.org/10.1039/B926326H

[43] Pace, C. N., Fu, H., Fryar, K. L., Landua, J., Trevino, S. R., Schell, D., Thurlkill, R. L., Imura, S., Scholtz, J. M., Gajiwala, K., Sevcik, J., Urbanikova, L., Myers, J. K., Takano, K., Hebert, E. J., Shirley, B. A., Grimsley, G. R. (2014). Contribution of hydrogen bonds to protein stability. Protein Science, 23(5), 652-661. https://doi.org/10.1002/pro.2449

[44] Ippolito, J. A., Christianson, D. W. (1992). The contribution of halogen atoms to protein–ligand interactions. International Journal of Biological Macromolecules,14(4),193-197. https://doi.org/10.1016/S0141-8130(05)80026-1

[45] Perrin, C. L. (2010). Are short, low-barrier hydrogen bonds unusually strong? Accounts of Chemical Research, 43(12), 1550-1557. https://doi.org/10.1021/ar100097j

[46] Cheng, F., Li, W., Liu, G., Tang, Y. (2013). In silico ADMET prediction: Recent advances, current challenges and future trends. Current Topics in Medicinal Chemistry, 13(10), 1273-1289. https://doi.org/10.2174/15680266113139990033